LAWRENCE
LIVERMORE
NATIONAL
LABORATORY

LLNL-JRNL-555712

DIXI (Dilation x-ray imager) a new/faster gated x-ray imager for the NIF

S. R. Nagel, T. J. Hilsabeck, P. M. Bell, D. K. Bradley, M. J. Ayers, M. A. Barrios, B. Felker, R. F. Smith, G. W. Collins, O. S. Jones, J. D. Kilkenny, T. Chung, K. Piston, K. S. Raman, B. Sammuli, J. D. Hares, A. K. L. Dymoke-Bradshaw

May 7, 2012

Physical Review of Scientific Insturments

Disclaimer

DIXI (Dilation x-ray imager) a new/faster gated x-ray imager for the NIF[a)]

S. R. Nagel[1, b)], T. J. Hilsabeck[2], P. M. Bell[1], D. K. Bradley[1], M.J. Ayers[1], M. A. Barrios[1], B. Felker[1], R. F. Smith[1], G. W. Collins[1], O. S. Jones[1], J. D. Kilkenny[2], T. Chung[2], K. Piston[1], K. S. Raman[1], B. Sammuli[2], J. D. Hares[3], A. K. L. Dymoke-Bradshaw[3]

[1]*Lawrence Livermore National Laboratory, 7000 East Avenue, Livermore, 94550, CA, USA*
[2]*General Atomics, P.O. Box 85608, San Diego, California 92186-5608, USA*
[3]*Kentech Instruments Ltd., Wallingford, Oxfordshire OX10, United Kingdom*

(Presented XXXXX; received XXXXX; accepted XXXXX; published online XXXXX)

As the yield on implosion shots increases it is expected that the peak x-ray emission reduces to a duration with a FWHM as short as 20 ps for ~7 10^{18} neutron yield. However, the temporal resolution of currently used gated x-ray imagers on the NIF is 40-100 ps. We discuss the benefits of the higher temporal resolution for the NIF and present performance measurements for DIXI, which utilizes pulse-dilation technology [1] to achieve x-ray imaging with temporal gate times below 10 ps. The measurements were conducted using the COMET laser, which is part of the Jupiter Laser Facility at the Lawrence Livermore National Laboratory.

I. INTRODUCTION

The performance of ICF targets relies on the symmetric implosion of DT fuel in order to form a uniform central hot spot with high enough areal density and temperature to achieve ignition[1]. Gated broadband x-ray imaging at energies exceeding ~8 keV is used to diagnose temporal (Δt = 40 to 100 ps) and spatial histories of the implosion symmetry and hot spot non-uniformities[2]. We will show that simulations predict features around bang time, which can only be resolved by faster gated imagers. Therefore it is important to diagnose those interactions at a higher frame rate.

Here we present data for a new x-ray imaging diagnostic, DIXI (Dilation x-ray imager), designed to work at shot neutron yields of up to 10^{17}. The diagnostic uses pulse-dilation of an electron signal to achieve temporal gate times of less than 10 ps. [3] Possible uses for this technology include: measuring high energy electron transport rates in fast ignition experiments, analyzing the symmetry of late stage implosion of high energy targets and investigating burn wave dynamics for igniting targets. In each case, it will be necessary to image the hard x-ray emission source (10-40 keV).

II. MODELING OF EXPECTED IMAGES WITH IMPROVED TEMPORAL RESOLUTION

Simulations of an igniting ICF capsule, which include alpha heating were conducted to model the expected difference in the images obtained by gated x-ray imagers with different temporal gate times. Rows 1-3 in figure 1 show the effect of different temporal resolutions with a spatial blurring of 10 µm. The image scales are 200 x 200 µm. A measurable difference in structure can be observed within 20 ps of bang time (0 ps) between the 40 ps an 10 ps gate times. For the 10 and 40 ps case the color scale on each image is normalized to the peak value on a given image. For the zero ps integration time the color scale is an absolute scale. This shows that the large increase in emission at 0 ps distorts the images between ±20 ps for the 40 ps gate. The fourth row in figure 1 shows the radiation temperature (T_{rad}, lhs) and the electron temperature (T_e, rhs). The contours that are plotted are the 17% contours, blue, white and red for 0 ps, 10 ps and 40 ps gate times respectively. It is easily observed that the 10 ps fast gate matched the contour better than the currently achievable 40 ps gate time.

III. INSTRUMENT DESCRIPTION

DIXI uses pulse dilation of an electron signal from a transmission Photo-Cathode (PC) to achieve the high temporal gate times. Figure 2(a) shows a diagram of DIXI indicating the main sections, whereas (b) illustrates the working principle of the instrument. An electron signal is generated as x-rays hit the Au or CsI transmission PC[4]. The electrons are sent through a drift space in which they are kept focused by a magnetic field. The magnetic field also de-magnifies the image. The dilated electrons then hit the gated MCP detector, which is followed by a phosphor, fiber block and CCD/film back (fiber bundle and recording media not shown). Because the PC is pulsed, the electron signal has a velocity distribution and the electrons created early in time have a larger energy. As this pulse traverses the drift space the signal is dilated. The MCP pulse is timed relative to the PC pulse to gate the electron signal. The electron arrival time at the MCP (τ) is the sum of the electron birth time (t), and the electron drift time. The electron drift time is dependent on the voltage of the PC pulse at the time the electron is born.

$$\tau(x,y,t) = t + \frac{L_{drift}(x,y)}{v_{drift}(x,y,t)}$$

$$v_{drift}(x,y,t) = \sqrt{2\,e\,V_{acc}(x,y,t)/m}$$

Where *(x,y)* is the birth location.

[a)]Contributed paper published as part of the Proceedings of the 19th Topical Conference on High-Temperature Plasma Diagnostics, Monterey, California, May, 2012.
[b)]Author to whom correspondence should be addressed: nagel7@llnl.gov.

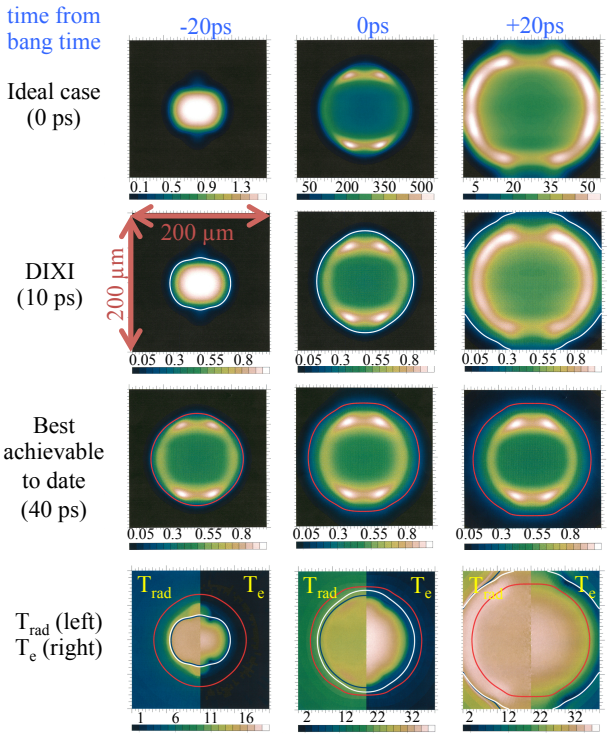

FIG. 1. (Color online). Rows 1-3 show the comparison of modeled x-ray pictures around bang time for different temporal integration times. The bottom row shows the radiation temperature (left) and the electron temperature (right) contours. The color bars are descriptive of the T_e contours (keV). Also shown are the simulated 17% contours for zero gate time (blue), a 10 ps gate (white) and a 40 ps gate (red).

The temporal resolution or gate width is determined by four parameters: drift length, MCP gate width, PC bias and the gradient of the fast PC pulse. Figure 3(a) shows how the gate width changes with PC bias for two different MCP gate widths, while the drift space and the PC pulse gradient are kept constant.

Apart from the temporal resolution the spatial resolution of the instrument at the detector (PC) plane is important. This depends on the material of the PC and the magnetic field strength at its position. Secondary photoelectrons are ejected with a characteristic energy spread depending on the PC material; CsI has a characteristic energy spread of 1.7 eV, compared to Au at 3.5 eV[4]. In the solenoid field the transverse excursion of the photoelectrons is limited to 4 times their cyclotron radius. [3]

$$4\,r_L[\mu m] = 95000\frac{\sqrt{T_e[\mathrm{eV}]}}{B[\mathrm{Gauss}]}$$

This shows that the spatial resolution is inversely proportional to the magnetic field at the PC. Another limiting factor on the spatial resolution of the instrument is the spatial resolution of the gated MCP detector, which is ~75 µm, which because of the de magnification by the magnetic field translates to 3x75 µm at the PC. Therefore the effective spatial resolution of the detector at the PC is a convolution of photoelectron orbits and MCP detector point spread function and is plotted in figure 3(b) for different magnetic fields and the two PC materials. On NIF, CsI will be used, as it not only shows better spatial resolution, but also has a higher yield of secondary electrons for the photon energies of interest[4]. First spatial resolution measurements are described below.

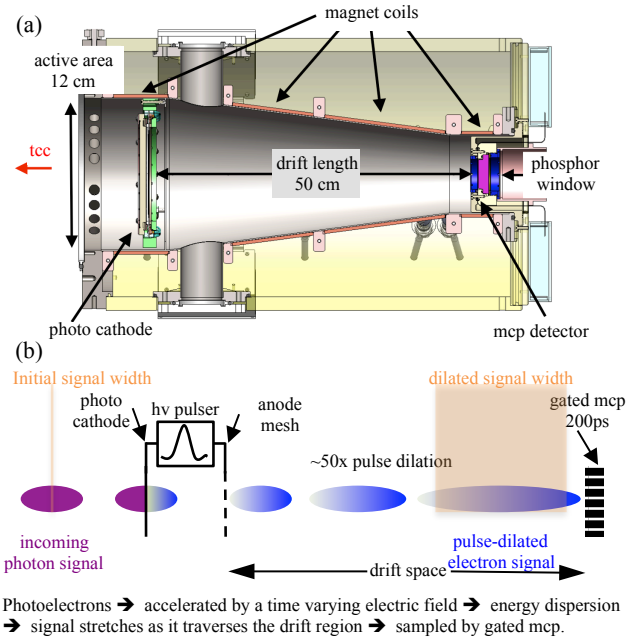

FIG. 2. (Color online). (a) DIXI schematic side view, optical fiber bundle and recording material not shown. (b) Working principle.

IV. PROPOSED EXPERIMENTAL SETUP ON NIF

On the NIF DIXI will be situated on the equatorial plane outside the target chamber (port 90/100). The imaging pinhole array is mounted inside the chamber at 10 cm from tcc. The resulting magnification of the images is 65x. A field of view of 150 µm at tcc (target chamber center) leads to a magnified image of ~9.8 mm in diameter. The delay on the inter-strip excitation voltage is adjustable for each of the four strips, and one strip is 120 mm long and has a time window ~250 ps. On NIF DIXI is titled down by 20 degrees from the horizontal, which shields the MCP detector from direct line of sight and enhances the shielding of the ccd camera. As the strips on the PC are oriented up-down, the tilt angle of the instrument changes the effective speed of the high voltage pulse across the PC to be 2.4 ps/mm. With the big image of ~10 mm, this means that the time difference between one edge of the field of view (FoV) to the other is ~24 ps. To enhance the temporal resolution two images separated in time by ~10 ps can be used to obtain a shorter gate time across the image. To be able to use this method for larger field of views, the jitter between strips has to be < 2 ps. The results of initial measurements are described in the next section.

V. EXPERIMENTAL VERIFICATION

The first x-ray tests of this instrument were conducted using the COMET laser at LLNL. The laser had a pulse duration of ~500-700 fs, a wavelength of 1.054 µm and a spot size of FWHM ~8 µm. This lead to laser intensities around ~2 10^{19} Wcm^{-2} that were focused onto a foil target 200 µm Cu or Zr foil target, coated with 2 µm Al. The generated x-rays had an unobstructed view to the instrument, which was run in pulsed mode, and the strips were nearly co-timed. A resulting raw image

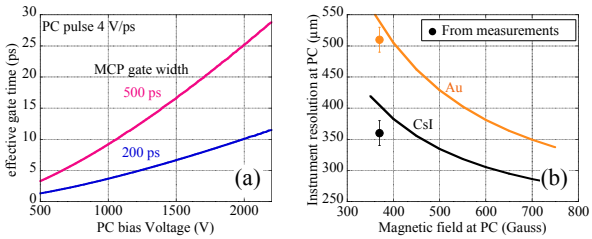

FIG. 3. (Color online) (a) Effective gate time plotted vs. the PC bias voltage for two different MCP gate widths. The drift length and gradient of the PC pulse were kept constant. (b) Instrument resolution at the PC plotted against magnetic field strength at the PC for two different PC materials (Au and CsI). The solid symbols show the experimentally measured (10-90% rise) spatial resolutions.

of the data can be seen in figure 4(a), where Au was used as the PC material. Figure 4(b) shows a lineout along one strip for a shot using a Zr target coated with Al and shows a x-ray pulse duration with FWHM ~6.6 ps. Here the PC material used was CsI. Taking into account a larger number of shots, the standard deviation of the strip to strip jitter between shots was measured to be <1 ps and the shortest signals measured were ~6.5 ps FWHM.

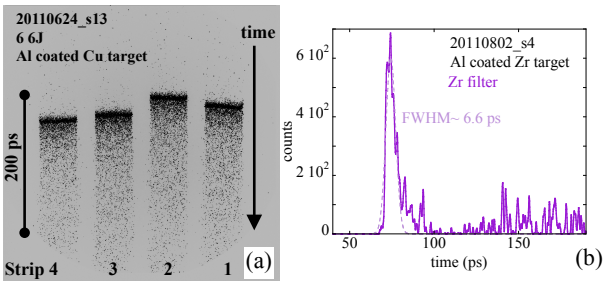

FIG. 4. (Color online). (a) Raw data image of example shot. (b) outline for Zr target shot with Gaussian fit to peak of the signal.

From these first x-ray tests the spatial resolution of the instrument for the two PC materials could also be measured. Measurements at 370 Gauss extraction field give a spatial resolution (10-90% rise) of 360 µm for the CsI PC, and 510 µm for the Au PC. Both cases are in good agreement with the theory, and are plotted in figure 3(b). Convolving this with the spatial resolution resulting from the pinhole imaging system (~660 µm (at PC) for 10 µm diameter pinholes with 65x) the total spatial resolution of the system using the CsI PC is 11.6 µm at tcc (752 µm at PC). To achieve a higher spatial resolution for the NIF the magnetic field strength will be increased.

Table 1 shows the values from a comparison measurement that was taken between DIXI and GXD[5] at COMET. The sensitivity is then compared to the ARIANE[6] detector, which is also located outside the NIF target chamber, in order to obtain an estimate of the expected events per resolution element and therefore the signal level anticipated when run on the NIF. The last row in table 1 assumes that as the pinholes for DIXI will be closer to tcc (10 cm) than the ARIANE pinholes (27 cm), increasing the observed solid angle. However this is counteracted by the shorter gate time. The comparison shows that the signal level on DIXI once situated outside the NIF target chamber and using 10 µm pinholes will be sufficient for shape analysis measurements.

TABLE I. DIXI should measure ~500 events/resolution element in the peak on NIF, Assuming that the Ω(DIXI) = 7Ω(ARIANE). (**) ARIANE was not installed on COMET, and the ARIANE COMET data was inferred from the assumption: GXD w\ 50V bias = ARIANE w\ 400V bias; (*) DC -750, 5kV Phosphor Pulse.

	gate width (ps)	cnts/ pixel	MCP bias (V)	CCD pixel /res	cnts/ event	events/ res element
DIXI COMET	5	1 k (strip4)	300	600	50 k	12
GXD COMET		3.1 k	50	900	8 k (*)	
ARIANE COMET	100	3 k (**)	400	900	20 k	135
ARIANE NIF	100	11 k	400	900	20 k	490
DIXI NIF	10	41 k				~500

VI. SUMMARY

Modeled images from ICF implosions that include alpha heating stress the need for better temporal resolution (~10 ps) gated x-ray framing cameras to observe the features of the implosion. We have shown that DIXI (Dilation x-ray imager) can be operated at a temporal resolution of <6 ps gate time, which will allow for the observation of these features that would not be visible with the currently available resolutions. The jitter between strips was measured to be < 1 ps, which is sufficient for the interleaved image method needed to obtain 10 ps gate time over the large images on the PC strip. A spatial resolution of ~ 360 µm was measured for a magnetic field of 370 Gauss at the PC, which will be increased for shots on the NIF to obtain a better spatial resolutions. First comparison measurements also show that the instrument is sensitive enough to be able to observe the implosion. DIXI was designed to work at neutron yields up to 10^{17}.

V ACKNOWLEDGMENTS

The Authors would like to acknowledge the support of the staff at the Jupiter Laser Facility and thank the Shape Group or providing the modeling results. Lawrence Livermore National Laboratory is operated by Lawrence Livermore National Security, LLC, for the U.S. Department of Energy, National Nuclear Security Administration under Contract No. DE-AC52-07NA27344. (LLNL-JRNL-555712)

VII. REFERENCES

[1] S. Atzeni and J. Meyer-ter Vehn, The Physics of Inertial Fusion, International Series of Monographs on Physics (Clarendon Press, Oxford, 2004); J. D. Lindl, Inertial Confinement Fusion: The Quest for Ignition and Energy Gain Using Indirect Drive (Springer-Verlag, New York, 1998).
[2] D. K. Bradley, P. M. Bell, O. L. Landen, J. D. Kilkenny, and J. Oertel, *Rev. Sci. Instrum.* **66**, 716 1995 .
[3] T.J. Hilsabeck *et al.*, *Rev. of Sci. Instrum.*, **81**, 10E317 (2010).
[4] B.L. Henke, J.P Knauer and K. Premaratne, *J. Appl. Phys.* **52**(3), 1509 (1981).
[5] J.A. Oertel *et al., Rev.of Sci. Instrum.*,**77**, 10E308 (2006)
[6] V. A. Smalyuk, *et. al., Proc. IEEE*, **8144,** 81440N (2011), submitted to SPIE